AGU PUBLICATIONS

JGR

Journal of Geophysical Research: Space Physics

RESEARCH ARTICLE
10.1002/2015JA021128

Special Section:
Low-Frequency Waves in Space Plasmas

Key Points:
- Propagation of ionospheric loop currents explained Pi2's in auroral zone
- Loop currents invoke wedge-like perturbations in midlatitudes
- Ionospheric loop currents accompany converging electric fields

Correspondence to:
O. Saka,
saka.o@nifty.com

Citation:
Saka, O., K. Hayashi, and A. S. Leonovich (2015), Explanation of Pi2 pulsations in auroral zone: Azimuthal propagation of ionospheric loop currents, *J. Geophys. Res. Space Physics*, *120*, doi:10.1002/2015JA021128.

Received 16 FEB 2015
Accepted 21 MAY 2015
Accepted article online 25 MAY 2015

©2015. American Geophysical Union. All Rights Reserved.

Explanation of Pi2 pulsations in auroral zone: Azimuthal propagation of ionospheric loop currents

O. Saka[1], K. Hayashi[2], and A. S. Leonovich[3]

[1]Office Geophysik, Ogoori, Japan, [2]Earth and Planetary Physics, University of Tokyo, Tokyo, Japan, [3]Institute of Solar-Terrestrial Physics, Siberian Branch of Russian Academy of Sciences, Irkutsk, Russia

Abstract The modes of Pi2 oscillations in space and on the ground, particularly in the auroral zone, have been discussed individually. The former is associated with the cavity oscillations either ideally trapped or partially trapped in the magnetosphere, and the latter is associated with the transient oscillations of the currents in the ionosphere. In this report, we show that ground polarization patterns (ellipticity and major axis orientation) of Pi2 pulsations in the nighttime sector from auroral zone to midlatitudes can be explained by the wave polarizations in the magnetosphere transmitted by the fundamental and the third harmonic deformations of the geomagnetic field lines. These ground polarization patterns are, however, understood alternatively as propagating large-scale ionospheric loop currents in auroral zone expanding ~1000 km longitudinally. One pattern propagates eastward in the dawn sector and the other westward in the dusk sector. The propagating loop currents for the generation of the ground polarizations were consistent with the vortical motion of auroras observed by all-sky imager in association with the Pi2 pulsations. Propagation of the ionospheric loop currents and vortical motion of auroras are a consequence of the Pi2-associated magnetosphere and ionosphere coupling through the Alfvén waves.

1. Introduction

Magnetometers in the auroral zone often record geomagnetic field oscillations in the frequency range of 5–20 mHz, with amplitudes exceeding 50 nT. These oscillations, referred to as substorm Pi2 pulsations, are related to the current oscillations of the auroral electrojet or the moving vortical currents induced in the ionosphere resulting from the coupling of the magnetosphere and ionosphere [*Olson and Rostoker*, 1975; *Pashin et al*., 1982; *Rostoker and Samson*, 1981; *Samson and Rostoker*, 1983; *Nishimura et al*., 2012]. The ground polarization characteristics (ellipticity and orientation of the major axis in *H-D* plane) of the Pi2 pulsations contain information on the source of Pi2 signals in the ionosphere and in the magnetosphere and mode of oscillations associated with the substorms. The polarization maps in *Samson and Harrold* [1983], derived from the magnetometer network in North America, presented the five-quadrant patterns of ellipticity and major axis orientations in the horizontal plane (*H-D* plane), covering from auroral zone to midlatitude over the nighttime sector spanning 5.3 magnetic local time. There were efforts to explain these polarization maps (ellipticity in particular) by the azimuth propagation of a pair of the field-aligned currents connected by the ionospheric Hall currents [*Samson*, 1982], or by a field line resonance [*Kuwashima*, 1978]. To explain the major axis orientations, oscillations of the field-aligned currents were used for both the midlatitude Pi2 pulsations [*Lester et al*., 1983; *Samson and Harrold*, 1983] and those at the eastern sector away from the westward traveling surge (WTS) [*Samson and Harrold*, 1983].

A statistical study on the geomagnetic field perturbations at the geosynchronous orbit revealed that the wave polarizations in Pi2 band (6–20 mHz) were polarized to counterclockwise (CCW) in the local time sector after 22:00 LT and clockwise (CW) in the local time sector before 22:00 LT viewed from above the equatorial plane [*Saka et al*., 2010]. Such polarization characteristics were correlated to the propagating directions of the auroral surge at the poleward boundary of auroral zone, referred to as poleward boundary aurora-surge (PBAS) [*Saka et al*., 2012a]. The PBAS propagated at 12–30 km/s at about 70°N and suggested an auroral manifestation of the flow diversions. On the ground, propagations of Pi2 pulsations in the auroral zone were diverted to the dayside, away from the center of the substorm current wedge typically at 20 km/s [*Samson and Harrold*, 1985]. We note that propagating velocities in the poleward boundary aurora surge and in the ground Pi2 pulsations were on the same order of magnitude. The

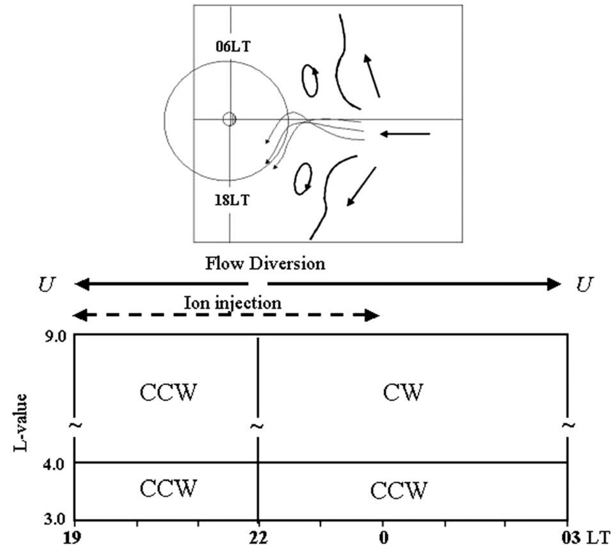

Figure 1. (top) Schematic illustration of the polarization ellipses in the equatorial plane (viewed from north) associated with surface waves generated by the flow diversions and injection trajectories with different particle energies (adapted from *Saka et al*. [2010]). (bottom) Patterns of the polarization ellipses in the equatorial plane (viewed parallel to the field lines) associated with the surface waves. The local time in the horizontal axis covered from 19:00 LT to 03:00 LT and an L in the vertical axis from 9 to 3, corresponding to 70°N to 55°N in invariant latitudes, respectively. The substorm ion injections expanded from 19:00 LT to 00:00 LT. The CCW quadrant in L = 3–4 is associated with the surface waves generated by the westward flows in the inner magnetosphere (see text). The LT represents the satellite's local time at the geosynchronous orbit.

east-west propagations are common features of the Pi2 pulsations on the ground and in auroras. If we assume that the wave polarizations in the magnetosphere are determined primarily by the flow diversions in the nighttime sector, the polarizations in the magnetosphere represent two-quadrant patterns, in contrast to the five-quadrant patterns on the ground. This report intends to demonstrate that the five-quadrant polarization maps on the ground and polarization patterns in the magnetosphere associated with the flow diversions are clearly connected.

2. Ellipticity Maps of Pi2 Pulsations

Geomagnetic field disturbances in Pi2 band (6–20 mHz) at geosynchronous orbit during the first 10 min intervals of Pi2 onset revealed that counterclockwise (CCW) rotation dominated before 22:00 LT switched to clockwise (CW) after 22:00 LT [*Saka et al*., 2010]. Here the wave rotations are viewed along the field lines. These disturbances were interpreted as surface waves excited in the nighttime sector by the surface displacement associated with the flow diversions [*Saka et al*., 2010]. The flow diversions occurred at 22:00 LT as illustrated in Figure 1 (top). The polarizations associated with the surface waves thus obtained are summarized in Figure 1 (bottom), with the flow diversions at 22:00 LT and ion injection regions from 19:00 to 00:00 LT [*Saka et al*., 2010]. To plot the polarization map in the bottom plot, we assumed that CCW polarizations were dominant in $L < 4$ associated with the westward propagating surface waves in the inner magnetosphere. Such assumptions match the midlatitude Pi2 pulsations where the westward propagations dominated [*Mier-Jedrzejowicz and Southwood*, 1979].

The wave polarizations associated with the surface waves were guided along the field lines by the fundamental harmonic except for the poleward part of the ion injection sector where the polarizations were guided by the third harmonic deformations in the meridian planes [*Saka et al*., 2012b]. Consequently, the field line rotations about the background field lines reversed in the poleward part of the ion injection sector. Figure 2 shows the resulting ground polarization patterns, where the reversed polarizations guided along the field lines are plotted in 65°N–70°N with CW from 19:00 LT to 22:00 LT and CCW from 22:00 LT to 00:00 LT. The footprints of geosynchronous satellites at 285° and at 252° for the magnetic field measurements were located 14 min west and 35 min east of the satellite meridian, respectively. The footprints of the satellite at 195° for particle measurements were 1.5 h east of the satellite meridian. Although the polarization patterns in the equatorial plane in Figure 1 were projected straightforwardly on the ground, the ion injection region may expand eastward to 01:00 LT of the ground local time.

The third harmonic deformations generate the westward Hall currents in the reversed polarization region [*Saka et al*., 2012b]. These westward Hall currents and eastward currents in lower latitudes by the fundamental harmonic close to form loop currents via meridional currents. The loop grew at the onset latitudes from small-scale (bead-like rippling) to the large-scale loop extending about 1000 km in east-west direction [*Saka et al*., 2014]. The polarization patterns in auroral zone can be interpreted alternatively by the propagation of these loop currents. Figure 3 illustrates the polarization patterns associated with the

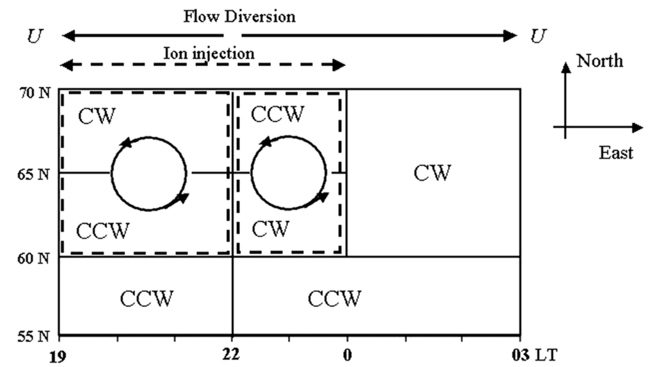

Figure 2. The ground mapping of the polarization ellipses in the equatorial plane. The polarization reversal in 65–70°N, 19:00–00:00 LT is associated with the third harmonic deformations of the geomagnetic fields in the meridian plane. The quadrants marked by dashed rectangles were explained by the propagating loop currents hypothesis (see text). The LT represents the ground local time.

propagating loop currents. Figure 3 (top) is for the loop currents closing CCW viewed from above the ionosphere, and Figure 3 (bottom) is for the loop closing CW. Each panel is subdivided according to the propagation directions; eastward to the right and westward to the left. There are four different types of the perturbations designated as Types A, B, C, and D. Type A and Type D show CW polarizations in the *H-D* plane, while Type B and Type C show CCW polarizations. Combinations of the propagation directions and the type of the perturbations uniquely determine the closing direction of the ionospheric loop

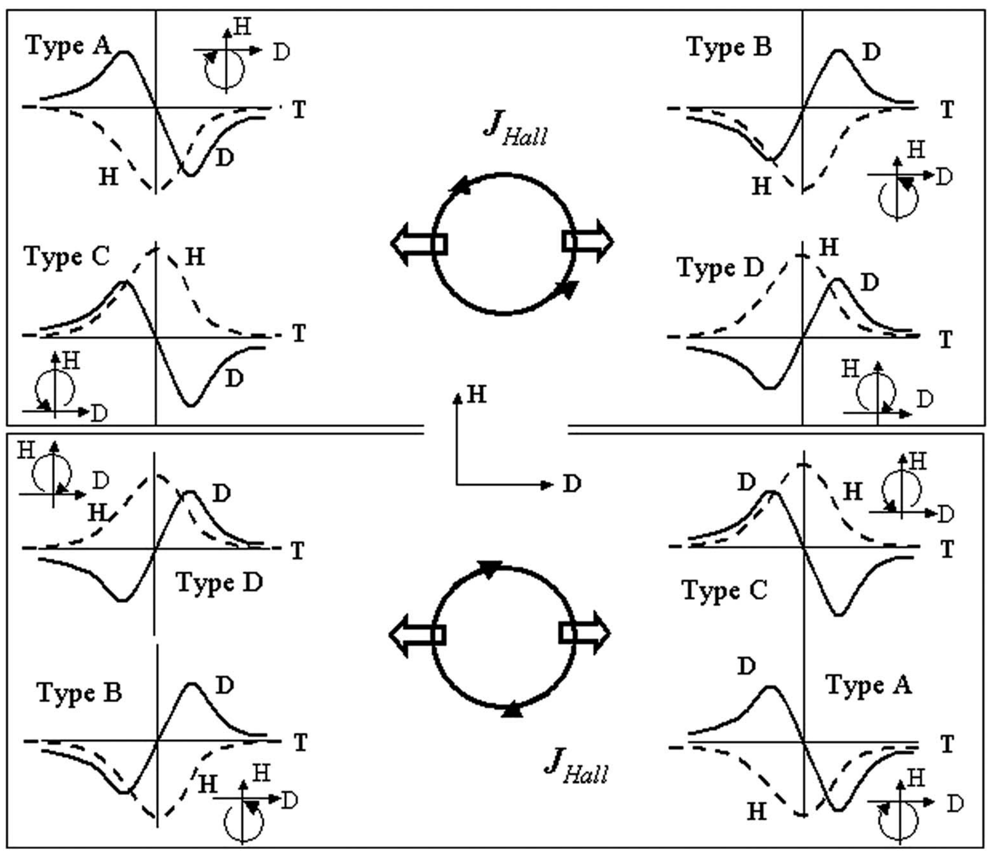

Figure 3. (top) Four-quadrant pattern of the waveforms on the ground (Types A, B, C, and D) and polarization ellipses in *H-D* plane associated with the propagating overhead loop currents. The currents closed CCW viewed from above the ionosphere. Each waveform represents the Pi2 pulse. The eastward propagation accompanied Type B to the north of the loop center and Type D to the south of the loop center. The westward propagation accompanied Type A to the north and Type C to the south. (bottom) Same as top plot but for loop current closing clockwise (CW) viewed from above the ionosphere. A combination of the propagation directions and the waveforms uniquely determines the rotation of the loop currents, either CW or CCW.

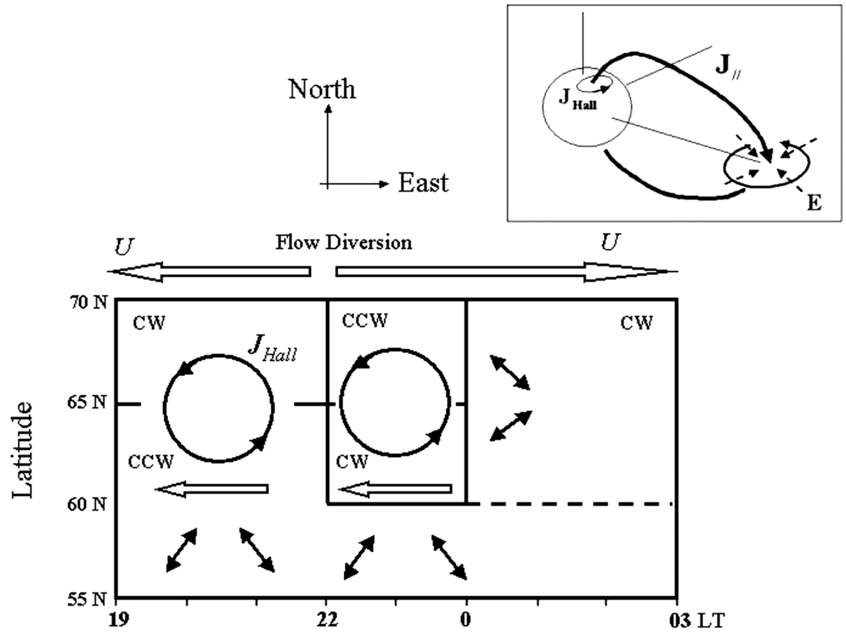

Figure 4. Ground polarization patterns covering 19:00 LT to 03:00 LT, and 70°N to 55°N in latitudes. The solid circles in 70–60°N are for the loop currents. The open arrows at the top and the middle denote the flow diversions at 22:00 LT and westward flows in the inner magnetosphere, respectively. The solid arrows illustrate major axis orientations for midlatitude Pi2 and Pi2 pulsations in the eastern sector of the auroral zone. The inset at the top right corner illustrates the coupling of the ionosphere and magnetosphere by a pair of the upward field-aligned currents ($J_{//}$) from the northern and southern hemispheres. The resulting plasma motions in the equatorial plane are shown as a solid circle, and converging electric fields are represented as *E* with dashed arrows.

currents, CW or CCW. Knowing that Pi2 pulsations change their *H* amplitudes from positive to negative with increasing latitudes [i.e., *Bjornsson et al.*, 1971], the loop closing CCW viewed from above the ionosphere can be adapted for the Pi2 pulsations (Figure 3 (top)). Those quadrants associated with the propagating loop currents are marked in Figure 2 by the dashed rectangles: westward propagating loop to the left (Type A for CW and Type C for CCW) and eastward propagating loop to the right (Type B for CCW and Type D for CW). The quadrants associated with the propagating loop were confined to the auroral zone (70–60°N). The center of the loop is located at 65°N where the *H* component switched the polarity.

3. Auroral Motions Associated With Pi2 Pulsations

The large-scale loop currents closing CCW viewed from above the ionosphere accompanied the converging electric fields, which generate the upward field-aligned currents from the center of the loop by the divergence of the Pedersen currents (we assumed uniform conductivity distributions in the ionosphere). A pair of upward field-aligned currents from the northern and southern hemispheres invoke the CW motion of plasmas in the equatorial plane [e.g., *Pashin et al.*, 1982]. The coupling of the ionosphere and the magnetosphere through the upward field-aligned currents can be regarded as a mapping of the ionospheric converging electric fields toward the equatorial plane. It is known that the equatorial continuity equation for flux tubes states that the flux tube content ($n\nu : \nu = \int ds/B$) in the frame of reference of the electric field drift is conserved if particle divergence arising from diamagnetic drift across the magnetic shell is neglected [*Lyons et al.*, 2003]. Assuming that the auroral luminosities were primarily related to flux tube content in the flux tube, the continuity equation states that motion of auroras follows the electric field drift in the magnetosphere. The brighter auroras are associated with the flux tube trajectories containing larger *n* and larger *B*. Larger *n* may enhance the precipitating flux accelerated at the lower latitudes, and larger *B* enhances the particle loss by increasing the loss cone angle. These trajectories can be interpreted as a wavefront of the Alfvén waves.

Inset at the top right corner of Figure 4 shows the converging electric fields and motion of plasmas in the equatorial plane associated with the upward field-aligned currents from the center of the ionospheric loop

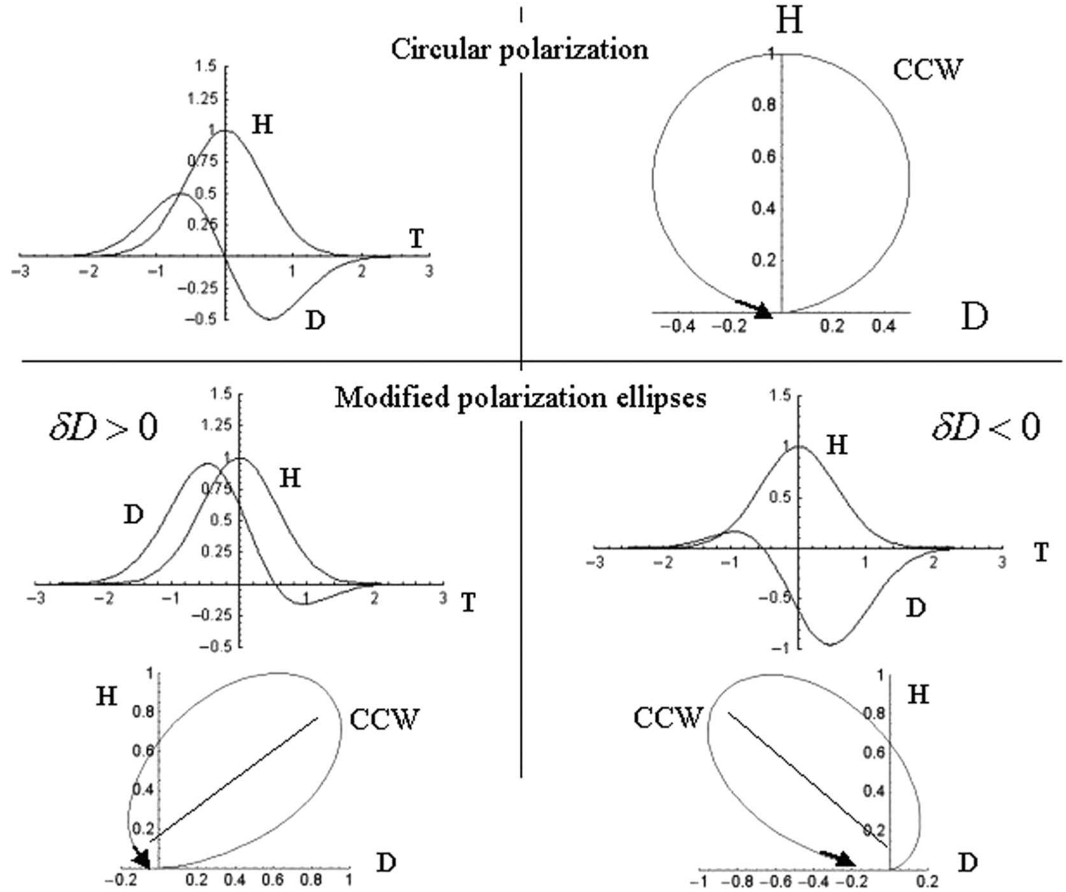

Figure 5. A modification of the circular polarized ellipse by imposing the offset pulse (δD) on the *D* component; $\delta D > 0$ in the bottom left and $\delta D < 0$ in the bottom right. The amplitudes of δD were 62% of the *D* amplitudes for the circular polarizations.

currents. The trajectories of the plasma motions in the equatorial plane correspond to the auroral motions in the ionosphere. The auroral motions may not complete the circle in general, because the flux tube content is not always conserved due to local pressure gradient (particle divergence). Consequently, only a part of the auroral motions rotating CW can be observed. The CW rotations of the auroras viewed from above the ionosphere are a common feature of the breakup auroras in global scales (westward traveling surge), midscale (fold), and in local scales (rayed structure of a sheet) [*Oguti*, 1975]. These auroral motions are referred to as S-structure formations. The converging electric fields also cause the global east-west flows in the equatorial plane. The westward flows generate the surface waves in the inner magnetosphere. These surface waves in the inner magnetosphere would correspond to the midlatitude Pi2 pulsations propagating westward with CCW polarizations. The eastward flows merge into the outer boundary flows, which is associated with the flow diversions occurring at 22:00 LT. Figure 4 summarized the polarization patterns of CW/CCW with flow diversions at 70°N (L = 9), a pair of the loop currents in the auroral zone (70–60°N, 19:00–00:00 LT), and westward flows at 60°N (L = 4). The flows in the magnetosphere and currents in the ionosphere were excited coherently in the Pi2 pulse.

4. Major Axis Orientation of Midlatitude Pi2 Pulsations

The rotation of the major axis is caused by the phase shift of the *D* component with respect to the *H* component or vice versa. Such phase shift can be obtained by introducing the amplitude offset in the *D* component, because the *D* component shows a bipolar waveform (see Figure 3). Using a single pulse, we demonstrate in Figure 5 how the *D* component offset associated with $+\delta D$ pulse, or $-\delta D$ pulse, modify the circular polarizations. The Pi2 waveform may be represented by the repetition of the pulse. Due to the offsets in the *D* component, the major axis points toward NE for the positive δD, while it points NW for the negative δD. The ellipticity did not change. For the calculation, the amplitudes of the δD pulse were 62% of the *D* amplitudes of the circular polarization. The decreasing amplitudes of the δD pulse rotated the major axis toward the north-south direction. If the loop currents in the auroral zone leaked to midlatitudes with ground perturbations of an order of nanotesla, the rotation of the major axis pointing to the center of the loop may occur at midlatitudes where Pi2 amplitudes are in few nanotesla [*Nishimura et al*., 2012; *Lester et al*., 1983]. The arrows in Figure 4 indicate the orientation of the major axis in the midlatitudes and in the sector east of the auroral zone. The orientations in the eastern sector are associated with the upward field-aligned currents of the loop currents. The orientation of the major axis with curvature pattern in the eastern quadrant and converging pattern in the midlatitude quadrant is reproduced in a manner consistent with the pattern shown in Figure 6 of *Samson and Harrold* [1983]. The opposite rotation of the major axis at the extreme end of the substorm current wedge [*Lester et al*., 1984] may also be associated with upward field-aligned currents and the current loop propagating westward in the western quadrants (see Figure 4).

5. Discussion

The maps of ground Pi2 polarizations in *Samson and Harrold* [1983] are shown in the substorm centered coordinates: the latitudes are relative to the center of the westward electrojet (WEJ) and the longitudes are relative to the center of the substorm current wedge. The latitudes covered +6° to −10° from the WEJ and −50° to 30° in longitude from the substorm center. There are five quadrants for the rotations of the polarization ellipse, both clockwise (CW) and counterclockwise (CCW) in the *H-D* plane. The following rotations of the polarization ellipse can be observed: two quadrants (CW/CCW) in the poleward region, and the other quadrants (CCW/CW) in the equatorward region of the WEJ; CW in the eastern sector; and CCW in the midlatitudes. WTS (westward traveling surge) was in the CW region at the substorm center. When the local time of the flow diversions (22:00 LT) corresponds to the −20° in longitudes and the center of the loop (65°N) to the WEJ (0°) in latitudes, ellipticity maps presented in Figure 7 of *Samson and Harrold* [1983] match the polarization patterns shown in Figure 4. Such correspondences indicate that the WTS and hence the substorm center is at 23:00 LT in the eastern sector of the flow diversion (eastward flows). The loop grew at the onset latitudes from small-scale vortical motions in the bead-like rippling [*Saka et al*., 2014]. The large-scale loop (~1000 km in east-west) completed within 4 min after the onset of the bead-like rippling. The intensifications of the ionospheric currents composing the current loop propagated to the east or to the west over ~1000 km in the auroral zone, which can be regarded on the ground as the propagation of the Pi2 pulsations. We suggest that the eastward propagating Pi2, in particular, accompanied the ionospheric loop currents expanding in latitudes to the poleward boundary of auroral zone, which may be observed as WTS by the ground magnetometer observations [*Samson and Rostoker*, 1983]. The western boundary of the loop would be expanding westward at velocities an order of magnitude smaller than the eastward propagation. In contrast to the eastward propagating loop, latitudinal expansions of the westward propagating loop may be suppressed by the reversed flows in the outer boundary associated with the flow diversions.

The westward plasma flows in the inner magnetosphere may be associated with the "equatorward expansion of aurora" [*Nakamura et al*., 1993]. The equatorward expansion may accompany the westward flows in lower latitudes in contrast to the eastward flows in higher latitudes for the poleward expansion. The corresponding westward flows in the equatorial plane generate the westward propagating surface waves observed as Pi2 pulsations in midlatitudes. Excitation of the loop currents at Pi2 periodicities may modify the ground polarizations in a manner consistent with the substorm current wedge. We suggest that the major axis orientations of the midlatitude Pi2 pulsations are not the oscillations of the overhead current itself but are associated with the phase modulations caused by the overhead currents (i.e., *Rostoker*, 1967).

We can describe the Pi2 pulsations in auroral zone in terms of the propagating converging electric fields. In the uniform conductivity distributions, the converging fields may have upward field-aligned currents at their center due to the divergence of the Pedersen currents and downward field-aligned currents in the periphery. The nonuniform distribution of the ionospheric conductivities may cause a separation of the field-aligned currents in longitudes to form a type of substorm current wedge [i.e., *Baumjohann et al*., 1981]. Although the nonuniform ionospheric conductivity distribution may skew the current pattern, we suggest that the propagating loop currents with the upward field-aligned currents at the center are a fundamental current system associated with the high-latitude Pi2 pulsations.

The onset latitudes of the Pi2 pulsations are worth noting. The equatorward drifts of the auroral arc from the poleward boundary of auroral zone are common features of the preonset auroras. These arcs are interpreted by the wavefront of the high-*m* Alfvén waves, where *m* is an azimuthal wave number [*Saka et al*., 2014, 2015]. They are generated as poloidal standing Alfvén waves by the variation of field-aligned currents flowing into or out of the ionosphere. These waves propagate across magnetic shells from the poloidal resonance surface to the toroidal surface, where the source frequency coincides with the eigenfrequency of toroidal Alfvén waves. The group velocity of these waves near the toroidal resonance surface is in the azimuthal direction and determines the main east-west movement direction of the auroral arcs related to them.

The Alfvén waves with $m \gg 1$ interact with the slow magnetosonic waves at the magnetic shells passing through the magnetotail current sheet. As a result, an original coupled mode of MHD-oscillation formed along the geomagnetic field lines, which has the properties of both the Alfvén and slow magnetosonic waves. In the preonset conditions the coupled modes become unstable (so-called "ballooning instability"), which may serve a trigger for the geomagnetic field reconnection process in the near-Earth part of the current sheet [*Liu*, 1997; *Leonovich and Kozlov*, 2014]. Like the usual poloidal Alfvén waves, the coupled modes propagate across the magnetic shells from the poloidal to the toroidal resonance surface, transforming gradually to the toroidal Alfvén waves.

The amplitude of unstable coupled modes also increases in such a propagation process. Therefore, start of the geomagnetic field reconnection process occurs most likely near toroidal resonance shells. As a result, the large-scale reconnection processes generate field-aligned currents closed through the ionospheric currents. Here these currents can be considered as large-scale geomagnetic Pi2 pulsations. They can be also regarded as an impulse of the Alfvén waves with m~1 that formed by the field-aligned current oscillations. From this point of view we can also understand moving of the vortical currents in the ionosphere in the east-west direction.

6. Summary

Polarization patterns of Pi2 pulsations (ellipticity and orientation of major axis) in high latitudes and in the midlatitudes were studied using the loop current hypothesis. The results obtained are as follows:

1. Substorm Pi2 pulsations using propagating loop current hypothesis explained the ground polarization maps of *Samson and Harrold* [1983].
2. The loop currents were accompanied by the upward field-aligned currents, which generated the converging electric fields in the magnetosphere and vortical motions in aurora.
3. Asymmetric developments arose in the ionospheric loop currents between those propagating to the east and to the west. The loop propagating eastward accompanied the WTS.
4. Polarizations of the midlatitude Pi2 pulsations are not oscillations of the overhead current itself but are modification of the polarization ellipses by the overhead currents.

Acknowledgments
The present study is based on the magnetometer data and the all-sky imager data from the Global Aurora Dynamics Campaign, STEP Polar Network (http://step-p.dyndns.org/~khay/).

Larry Kepko thanks the reviewers for their assistance in evaluating this paper.

References

Baumjohann, W., R. J. Pellinen, H. J. Opgenoorth, and E. Nielsen (1981), Joint two-dimensional observations of ground magnetic and ionospheric electric fields associated with auroral zone currents: Current systems associated with local auroral break-ups, *Planet. Space Sci.*, *29*, 431–447.

Bjornsson, A., O. Hillebrand, and H. Voelker (1971), First observational results of geomagnetic Pi2 and Pc5 pulsations on a north-south profile through Europe, *Z. Geophys.*, *37*, 1031–1042.

Kuwashima, M. (1978), Wave characteristics of magnetic Pi2 pulsations in the auroral region-spectral and polarization studies, *Mem. Natl. Inst. Polar Res., Ser. A, Aeron.*, *15*, 1–79.

Leonovich, A. S., and D. A. Kozlov (2014), Coupled guided modes in the magnetotails: spatial structure and ballooning instability, *Astrophys. Space Sci.*, *353*, 9–23.

Lester, M., W. J. Hughes, and H. Singer (1983), Polarization patterns of Pi2 pulsations and the substorm current wedge, *J. Geophys. Res.*, *88*, 7958–7966, doi:10.1029/JA088iA10p07958.

Lester, M., W. J. Hughes, and H. Singer (1984), Longitudinal structure in Pi2 pulsations and the substorm current wedge, *J. Geophys. Res.*, *89*, 5489–5494, doi:10.1029/JA089iA07p05489.

Liu, W. W. (1997), Physics of the explosive growth phase: Ballooning instability revisited, *J. Geophys. Res.*, *102*, 4927–4931, doi:10.1029/96JA03561.

Lyons, L. R., C.-P. Wang, and T. Nagai (2003), Substorm onset by plasma sheet divergence, *J. Geophys. Res.*, *108*(A12), 1427, doi:10.1029/2003JA010178.

Mier-Jedrzejowicz, W. A. C., and D. J. Southwood (1979), The east-west structure of mid-latitude geomagnetic pulsations in the 8–25 mHz band, *Planet. Space Sci.*, *27*, 617–630.

Nakamura, R., T. Oguti, T. Yamamoto, and S. Kokubun (1993), Equatorward and poleward expansion of the auroras during auroral substorm, *J. Geophys. Res.*, *98*, 5743–5759, doi:10.1029/92JA02230.

Nishimura, Y., L. R. Lyons, T. Kikuchi, V. Angelopoulos, E. Donovan, S. Mende, P. J. Chi, and T. Nagatsuma (2012), Formation of substorm Pi2: A coherent response to auroral streamers and currents, *J. Geophys. Res.*, *117*, A09218, doi:10.1029/2012JA017889.

Oguti, T. (1975), Metamorphoses of aurora, *Mem. Natl. Inst. Polar Res., Ser. A, Aeron.*, 1–101.

Olson, J. V., and G. Rostoker (1975), Pi2 pulsations and the auroral electrojet, *Planet. Space Sci.*, *23*, 1129–1139.

Pashin, A. B., K. H. Glassmeier, W. Baumjohann, O. M. Raspopov, A. G. Yahnin, H. J. Opgenoorth, and R. J. Pellinen (1982), Pi2 magnetic pulsations, auroral break-ups, and the substorm current wedge: A case study, *J. Geophys.*, *51*, 223–233.

Rostoker, G. (1967), The polarization characteristics of Pi2 micropulsations and their relation to the determination of possible source mechanisms for the production of nighttime impulsive micropulsation activity, *Can. J. Phys.*, *45*, 1319–1335.

Rostoker, G., and J. C. Samson (1981), Polarization characteristics of Pi2 pulsations and implications for their source mechanisms: Location of source regions with respect to the auroral electrojet, *Planet. Space Sci.*, *29*, 225–247.

Saka, O., K. Hayashi, and M. Thomsen (2010), First 10 min intervals of Pi2 onset at geosynchronous altitudes during the expansion of energetic ion regions in the nighttime sector, *J. Atmos. Sol. Terr. Phys.*, *72*, 1100–1109.

Saka, O., K. Hayashi, and D. Koga (2012a), Periodic aurora surge propagating eastward/westward at poleward boundary of aurora zone during the first 10 min intervals of Pi2 onset, *J. Atmos. Sol. Terr. Phys.*, *80*, 285–295, doi:10.1016/j.jastp.2012.02.010.

Saka, O., K. Hayashi, and D. Koga (2012b), Excitation of the third harmonic mode in meridian planes for Pi2 in the auroral zone, *J. Geophys. Res.*, *117*, A12215, doi:10.1029/2012JA018003.

Saka, O., K. Hayashi, and M. Thomsen (2014), Pre-onset auroral signatures and subsequent development of substorm auroras: A development of ionospheric loop currents at the onset latitudes, *Ann. Geophys.*, *32*, 1011–1023.

Saka, O., K. Hayashi, and A. S. Leonovich (2015), Ionospheric loop currents and associated ULF oscillations at geosynchronous altitudes during pre-onset intervals of substorm aurora, *J. Geophys. Res. Space Physics*, doi:10.1002/2014JA020842.

Samson, J. (1982), Pi2 pulsations: High latitude results, *Planet. Space Sci.*, *30*, 1239–1247.

Samson, J. C., and B. G. Harrold (1983), Maps of the polarizations of high latitude Pi2's, *J. Geophys. Res.*, *88*, 5736–5744, doi:10.1029/JA088iA07p05736.

Samson, J. C., and B. G. Harrold (1985), Characteristic time constants and velocities of high-latitude Pi2's, *J. Geophys. Res.*, *90*, 12,173–12,181, doi:10.1029/JA090iA12p12173.

Samson, J. C., and G. Rostoker (1983), Polarization characteristics of Pi2 pulsations and implications for their source mechanisms: Influence of the westward traveling surge, *Planet. Space Sci.*, *31*, 435–458.